FORECASTING OF OUTDOOR THERMAL COMFORT INDEX IN URBAN OPEN SPACES
The Nis Fortress Case Study

by

Ivana S. BOGDANOVIĆ PROTIĆ[a]*, Ana V. VUKADINOVIĆ[b], Jasmina M. RADOSAVLJEVIĆ[b], Meysam ALIZAMIR[c], and Mihajlo P. MITKOVIĆ[a]

[a] Faculty of Civil Engineering and Architecture, University of Nis, Nis, Serbia
[b] Faculty of Occupational Safety, University of Nis, Nis, Serbia
[c] Young Researchers and Elites Club, Hamedan Branch, Islamic Azad University, Hamedan, Iran

Original scientific paper
DOI: 10.2298/TSCI16S5531B

Outdoor thermal environment is affected by variables like air temperature, wind velocity, humidity, temperature of the radiant surfaces, and solar radiation, which can be expressed by a single number – the thermal index. Since these variables are subject to annual and diurnal variations, prediction of thermal comfort is of special importance for people to plan their outdoor activities. The purpose of this research was to develop and apply the extreme learning machine for forecasting physiological equivalent temperature values. The results of the extreme learning machine model were compared with genetic programming and artificial neural network. The reliability of the computational models was accessed based on simulation results and using several statistical indicators. According to obtained results, it can be concluded that extreme learning machine can be utilized effectively in short term forecasting of physiological equivalent temperature.

Key words: *thermal comfort, urban open spaces, extreme learning machine, physiological equivalent temperature, prediction,*

Introduction

In recent years there has been a growing interest in linking urban planning, environmental health, and the quality of life [1]. Public open spaces have been recognized as an opportunity to provide a healthy environment for city dwellers. Pleasant thermal conditions allow longer duration of stay of users of urban open spaces, which can contribute to health, relaxation, socialization, and entertainment of children and adults. The frequency of usage of urban open spaces is strongly affected by the relation between microclimatic conditions of urban open spaces and human comfort, so this relation must be taken into consideration during urban design and planning [2]. In order to describe and assess human thermal comfort, Gagge, Hill, and Barnard developed the concept of thermal index at the beginning of the 20th century [3]. The possibility to assess the human thermal condition by a single number which integrates all relevant parameters was first recognized by Fanger in 1972 [4]. Since then, more than 40 indices were developed and some of the most frequently used ones are predicted mean

* Corresponding author; e-mail: ivanab76@yahoo.com

vote (PMV), physiologically equivalent temperature (PET), standard effective temperature (SET), and perceived temperature (PT) [5]. The PET was introduced by Hoppe and Mayer and it represents an equivalent to the air temperature at which the heat balance of the human body is maintained with core and skin temperatures equal to those under the conditions being assessed. Numerous studies in outdoor thermal comfort assessment, which included PET, were conducted for different climatic regions and areas, such as Greece [4], Iran [5], Italy [6], Spain [7], and others.

While most previous studies were focused on finding the proper way of selecting and further incorporating the number of influencing factors into the thermal comfort index models [8], there is an evident lack of investigations where prediction of the thermal index was analyzed. We assert that predicted outdoor thermal comfort index should be regarded as an additional useful parameter, besides predicted outdoor temperature, for planning city dwellers' activities in outdoor spaces. Therefore, the aim of the present study is to develop and assess performances of predictive models of outdoor thermal comfort index. Starting from the assumption that the observed data were created as a result of a nonlinear stochastic underlying process, the focus was solely on soft computing methods. Three methods were used for creating predictive models: (1) extreme learning machine (ELM), (2) single layer feedforward artificial neural network (ANN), and (3) genetic algorithm (GA). Predictive models were based on experimentally acquired data in the Nis Fortress, Serbia, a popular outdoor recreational open space for the citizens of Nis. Models were developed for a predictive horizon of 1 hour (6 steps ahead) and predictive results were subsequently compared.

Research methodology

Experimental procedures

Study area

The City of Nis, the third largest city in Serbia (43 ° 19 ' 32 " SG W, 21 ° 53' 43 " E) is located in the Nis basin, at an average altitude of 196 m. It is the third largest city in Serbia with a population of 256,000. The administrative area of the City of Nis is 596.71 km^2. The Nis Fortress is an urban fortress in downtown Nis on the right bank of the Nisava River, which has a continuity of about two millennia of continuous existence, as evidenced by numerous archaeological findings. By its present condition, it is one of the best preserved fortifications of this type in Serbia and the Balkan Peninsula.

In addition to the historical and cultural significance, this fortress is an important outdoor recreational open space – one of the city's major parks. It has an area of about 220,000 m^2. The site is dominated by green areas, grassland, bushes, and trees. The rest of the area is covered in paved paths, children's playgrounds, and several buildings with different purposes (fig. 1). The park is used every day and on weekends, which is aided by the excellent transport links with other parts of the city. In the spatial-functional terms, the fortress has a wide range of potential for successful organization of leisure activities: walking, recreational activities, child play, as well as rest and relaxation. Typical patterns of recreational activities in the fortress are shown in fig. 2.

The multi-character of the fortress contributes to the high frequency of visits to this city park. The special significance of this city park is reflected in the environmental and health benefits – creating optimal conditions for rest, refreshment, and recovery of the body in physiological and psychological terms. The particular importance of this urban open space

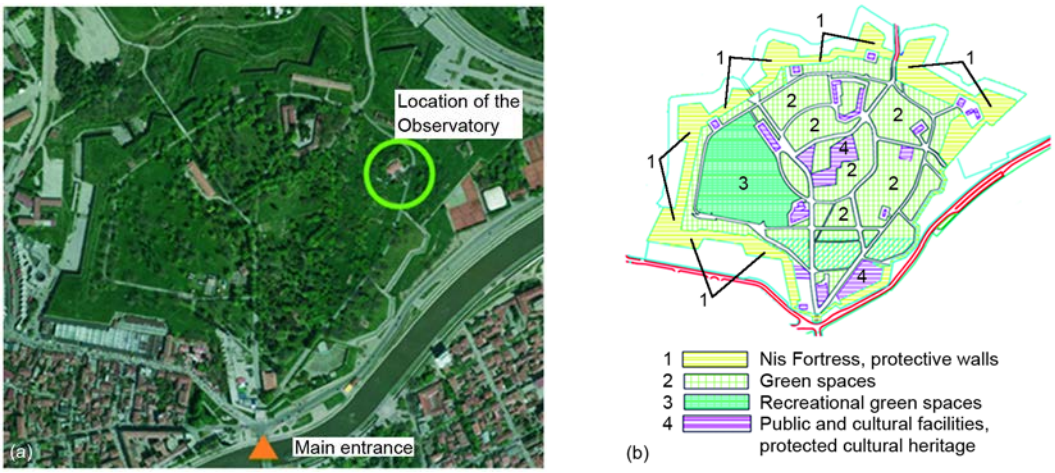

Figure 1. (a) Location of the study site in the Nis Fortress. The circle indicates a Meteorological station [9], (b) Land use of the study area [10]

Figure 2. Pictures of the study site [11]

can be seen in the context of its providing opportunities for recreational activities which can compensate for an increasing lack of physical activity of citizens in their everyday life, extended working hours, as well as physical and mental stresses which are due to the different types of efforts. This is particularly important in the current conditions of global climate

change, negative impact of urban air pollution, and reduction of vacant space in the City of Nis, in line with the current trend of usurping open spaces for constructing buildings for profit. At the same time, this fortress provides adequate space for socialization and citizen gatherings, and the deepening of interpersonal relationships, in contrast to the growing tendency of human alienation and domination of virtual friendships through social networks. The green areas, as a dominant cover of this urban open space, improve the chemical composition of air, filter it, and contribute to the air pollution reduction and gaseous pollutants and heavy metals absorption. In this context, the aim of this study is prediction of thermal comfort in the Nis Fortress, as the main city park, in order to be the preferred destination for citizens.

The PET and RayMan model

In this study we used PET, which is a thermal index recommended by the German Association of Engineers and officially used by the German Meteorological Service. The PET index was derived from the human energy balance expressed in [°C] and it is suitable for urban and regional planners because of the simplicity of interpretation. Additional advantage of PET is that it can be used not only for summer conditions, but throughout the year. The PET index calculation was performed using the RayMan model developed by Matzarakis [12]. The RayMan model is based on the German VDI-Guidelines 3789 (interactions between atmosphere and surfaces; calculation of short- and long-wave radiation) and VDI-Guidelines 3787 (methods for the human-biometeorological evaluation of climate and air quality for urban and regional planning) [12].

The Rayman model has a user-friendly interface and can be applied not only by experts in human-biometeorology, but also by people with less experience in this field of science. The final output of the Rayman model is calculated mean radiant temperature (T_{mrt}), the most important biometeorological parameter which is required in the energy balance model for humans and thus for the assessment of urban bioclimate and the resulting thermal indices. To calculate radiant fluxes and common thermal indices, the Rayman model requires basic meteorological data such as air temperature, air humidity and wind speed, and other input data like the sky view factor, albedo, and emissivity of the surrounding surfaces. Simulation of T_{mrt} using the Rayman model was validated through experimental data and it showed that the estimated values of T_{mrt} and the data driven from direct measurements were in high agreement [12]. For the calculation of mean radiant temperature this model uses the equations [12]:

$$T_{\mathrm{mrt}} = \left[\frac{1}{\sigma} \sum_{i=1}^{n} \left(E_i + a_k \frac{D_i}{\varepsilon_p} \right) F_i \right]^{0.25} \tag{1}$$

where σ is the Stefan-Boltzmann constant (= $5.67 \cdot 10^{-8}$ W/m^{2}K^4), and ε_p – the emission coefficient of the human body (standard value 0.97), D_i – the diffuse solar radiation and the diffusely reflected global radiation, and a_k – the absorption coefficient of the irradiated body surface area of short-wave radiation:

$$T_{\mathrm{mrt}}^{*} = \left[T_{\mathrm{мрт}}^{4} + \frac{f_p a_k I^{*}}{\varepsilon_p \sigma} \right]^{0.25} \tag{2}$$

where I* is the radiation intensity of the Sun on a surface perpendicular to the incident radiation direction [12].

Experimental set-up

The data used for development of predictive models were collected at the Nis Observatory (21°54E, 43°20N, altitude 202 m), a part of the Meteorological Observation System of Serbia (MOSS). The observatory is located inside the study area and its location is shown in fig. 1. Meteorological data was collected from an automatic weather station. Global radiation was measured with CMP6 pyranometer from Kipp & Zonen (fully compliant with ISO 9060:1990 specification for a first class pyranometer, for measuring global solar radiation (Spectral range: 285 to 2800 nm, sensitivity: 5 to 20 μV/W/m²), fig. 3(a). Air temperature was measured with temperature sensor PT 100 (Operating temperature range: –65 °C to +70 °C, operating humidity range: 0 to 100%, Accuracy class 1/5 DIN: ±0.1 °C). Relative humidity was measured with HygroClip 2 HC2-S3C03-PT15 (Accuracy: ±1.0 %RH), fig. 3(b).

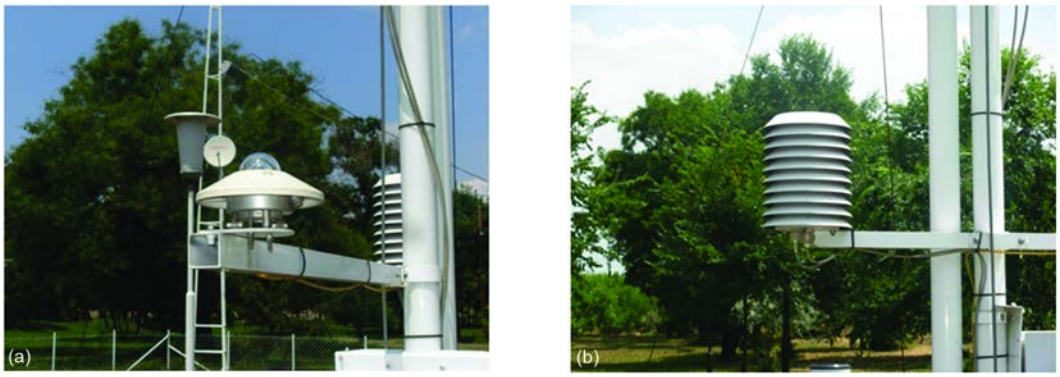

Figure 3. (a) The CMP6 pyranometer, (b) PT 100 temperature sensor and HygroClip 2 HC2-S3C03-PT15

Data

Input parameters for PET calculation were air temperature, vapor pressure, wind speed, and global radiation. Data were taken at 1 min sampling resolution during July and August 2014. Afterwards, data were averaged to 10 min values. For the thermo-physiological parameter of the human body we used a typical 35 year-old male, 1.75 m tall, weighing 75 kg, with a clothing index of 0.9 and the level of activity 80 W. The output variable was PET (t + 6), *i. e.* the value of physiologically equivalent temperature 6 steps ahead (predictive horizon of one hour). Descriptive statistics for relevant variables are provided in tab. 1.

Table 1. Summary statistics of input data

Inputs	Parameters description	Average	Maximum	Minimum	Standard deviation
Input 1	Air temperature, T_a, [°C]	21.9	35.3	9.2	4.83
Input 2	Vapor pressure, *VP*, [hPa]	17.1	25.2	10.0	2.73
Input 3	Wind speed, W_s, [ms^{-1}]	1.1	7.1	0.0	0.79
Input 4	Global radiation, R_s, [Wm^{-2}]	252.0	1102.7	0.0	317.22
Input 5	Physiological equivalent temperature	21.9	48.3	3.6	9.97

Finally, six time series (five input and one output) were created, each with 8.883 observations. These series were used for subsequent model development and testing. Training

and testing data were divided in a 70/30 ratio. Model parameters were estimated using the five-fold cross validation on training data sets. The test set was not used for model building. It was solely used for assessing predictive performances of models.

Extreme learning machine

Huang *et al.* [13, 14] developed extreme learning machine (ELM) as a novel learning algorithm for single hidden layer feedforward networks (SLFN).

According to the authors, this approach has notable advantages as compared with conventional neural networks as follows: (1) the ELM is easy to use, offers fast training, and also produces good generalization results [13, 14]; (2) in conventional neural networks all the parameters of the networks, such as learning rate, learning epochs, and local minima, are tuned iteratively by using such learning algorithms, and (3) the ELM can be easily implemented and can obtain the smallest training error and the smallest norm of weights [13, 14].

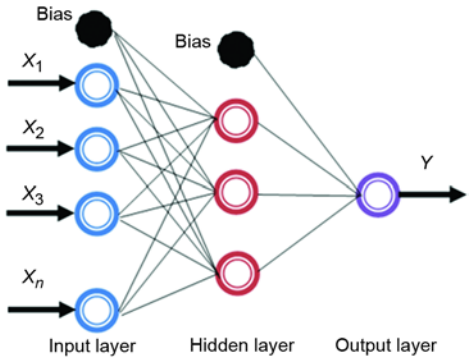

Figure 4. The topological structure of the extreme learning machine network used in this study

Figure 4 shows the schematic topological structure of ELM network. For M arbitrary input-output samples $(\vec{x}_i, \vec{t}_i)$, where $\vec{x}_i = [x_{i1}, x_{i2}, \ldots, x_{in}]^T \in \vec{R}^n$ and $\vec{t}_i = [t_{i1}, t_{i2}, \ldots, t_{in}]^T \in \vec{R}^m$, standard single hidden layer feedforward networks (SLFN) with N hidden nodes and activation function $g(x)$ are modeled [13, 14]:

$$\sum_{i=1}^{M} \vec{\beta}_i g_i(\vec{x}_j) = \sum_{i=1}^{M} \vec{\beta}_i g(\vec{w}_i \vec{x}_j + b_i) = o_j, \qquad j = 1, ..., N \tag{3}$$

where $\vec{w}_i = [w_{i1}, w_{i2}, \ldots, w_{in}]^T$ is the weight vector between input and hidden nodes, $\vec{\beta}_i = [\beta_{i1}, \beta_{i2}, \ldots, \beta_{in}]^T$ is the weight vector between output and hidden nodes, and b_i is the threshold of the i^{th} hidden node. The standard single hidden layer feedforward networks with M hidden nodes with activation function $g(x)$ are modeled [13, 14]:

$$\sum_{i=1}^{M} \vec{\beta}_i g(\vec{w}_i \vec{x}_j + b_i) = \vec{t}_j, \qquad j = 1, ..., N \tag{4}$$

These equations can be written [13, 14]:

$$\mathrm{H}\beta = \mathrm{T} \tag{5}$$

where

$$[\mathrm{H}] = \begin{bmatrix} g(\vec{w}_1 \vec{x}_1 + b_1) & \cdots & g(\vec{w}_M \vec{x}_1 + b_M) \\ \vdots & \cdots & \vdots \\ g(\vec{w}_1 \vec{x}_N + b_1) & \cdots & g(\vec{w}_M \vec{x}_N + b_M) \end{bmatrix}_{NM}$$

$$[\beta] = \begin{bmatrix} \beta_1^T \\ \vdots \\ \beta_M^T \end{bmatrix}_{Mm} \quad \text{and} \quad [\mathrm{T}] = \begin{bmatrix} t_1^T \\ \vdots \\ t_M^T \end{bmatrix}_{Nm}$$

where [H] is the hidden layer output matrix on neural network. The output weights can be constructed using the following equation:

$$\beta = [H^{\dagger}]\,[T] \tag{6}$$

where $[H^{\dagger}]$ is the Moore-Penrose generalized inverse of the hidden layer output matrix [H].

Models performance evaluation

Predictive performances of the proposed models were assessed using the following criteria: the root mean square error (RMSE), coefficient of determination (R^2), and Pearson coefficient (r). These statistics are defined:

– root-mean-square error (RMSE),
– Pearson correlation coefficient (r), and
– coefficient of determination (R^2).

$$\mathrm{RMSE} = \sqrt{\frac{\sum_{i=1}^{n}(P_i - O_i)^2}{n}} \tag{7}$$

$$r = \frac{n\left(\sum_{i=1}^{n} O_i P_i\right) - \left(\sum_{i=1}^{n} O_i\right)\left(\sum_{i=1}^{n} P_i\right)}{\sqrt{\left[n\sum_{i=1}^{n} O_i^2 - \left(\sum_{i=1}^{n} O_i\right)^2\right]\left[n\sum_{i=1}^{n} P_i^2 - \left(\sum_{i=1}^{n} P_i\right)^2\right]}} \tag{8}$$

$$R^2 = \frac{\left[\sum_{i=1}^{n}\left(O_i - \overline{O_i}\right)\left(P_i - \overline{P_i}\right)\right]^2}{\sum_{i=1}^{n}\left(O_i - \overline{O_i}\right)\sum_{i=1}^{n}\left(P_i - \overline{P_i}\right)} \tag{9}$$

where O_i and P_i represent the observed and predicted values of PET, respectively, and n – the number of samples.

Results and discussion

Performance analysis

In this section, performance results of the ELM predictive model are reported. Figure 5 presents the accuracy of the developed ELM predictive model for PET based on training and testing data. The prediction accuracy is acceptable for these data. It can be seen that most of the points fall along the diagonal line. It follows that the prediction results with ELM method are in high agreement with the observed values. This statement can be additionally confirmed with acceptable value for the coefficient of determination. The number of overestimated or underestimated values is limited. Consequently, it is obvious that the predictive model has acceptable precision.

Additionally, predictive results of ANN and GP models are presented in figs. 6 and 7.

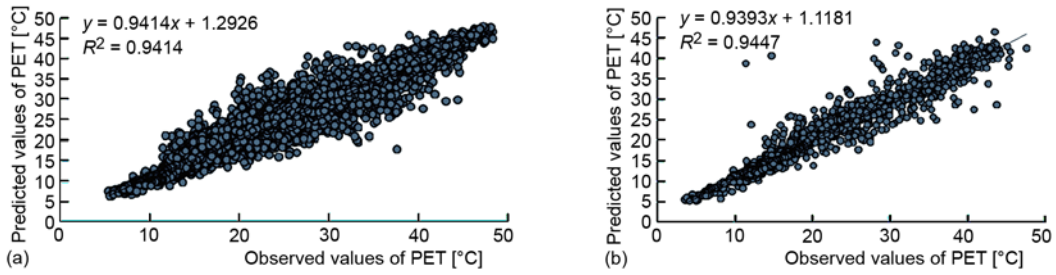

Figure 5. Scatter plots of actual and forecasted values of PET using the ELM approach for (a) training and (b) testing data

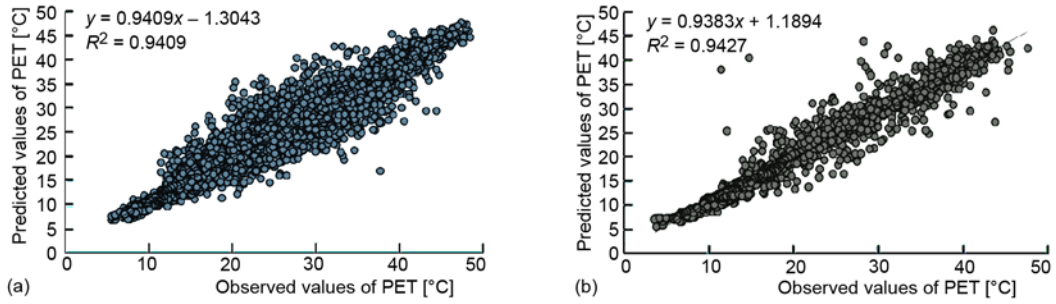

Figure 6. Scatter plots of actual and forecasted values of PET using the ANN approach for (a) training and (b) testing data

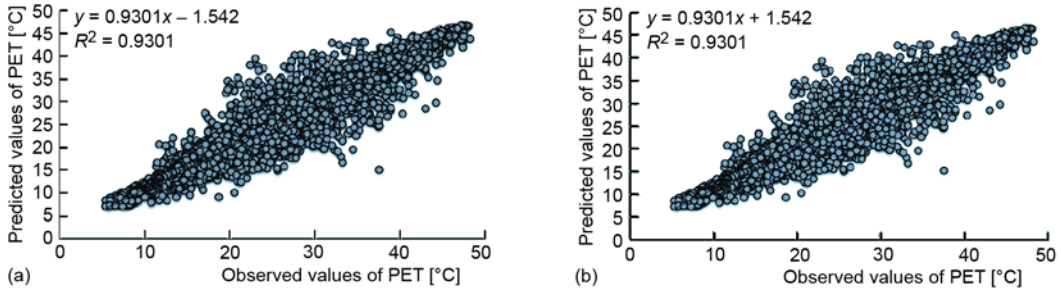

Figure 7. Scatter plots of actual and forecasted values of PET using the GP approach for (a) training and (b) testing data

Performance comparison of ELM, ANN, and GP

Prediction results of ELM, ANN, and GP models are shown in tabs. 2 and 3. The results for training and test set of data are presented. Again, the conventional statistical error indicators (RMSE, r, and R^2) were used for comparison.

Table 2. Comparative performance statistics of the ELM, ANN, and GP models for PET prediction (training set of data)

ELM (training)			ANN (training)			GP (training)		
RMSE	R^2	r	RMSE	R^2	r	RMSE	R^2	r
2.398342	0.9447	0.97025	2.40753	0.9427	0.970019	2.61878	0.9324	0.964425

Table 3. Comparative performance statistics of the ELM, ANN, and GP models for PET prediction (testing set of data)

ELM (testing)			ANN (testing)			GP (testing)		
RMSE	R^2	r	RMSE	R^2	r	RMSE	R^2	r
2.402102	0.9414	0.97197	2.442757	0.9409	0.970919	2.650716	0.9301	0.965604

Based on the results from tabs. 2 and 3, it can be concluded that the best prediction performances were obtained with the ELM model ($RMSE_{ELM}$ = 2.398342, $RMSE_{ANN}$ = = 2.40753, and $RMSE_{GP}$ = 2.61878). Additionally, it is obvious that the difference between error of prediction for training and testing sets of data is the lowest in the case of the ELM method. This proves that the ELM method has the best generalization ability.

Conclusion

Forecasting the future PET values is intricate, considering that this index incorporates many indicators and factors. In the present study, we described the prediction of PET index using the ELM method. An efficient prediction model, based on four input parameter, was deployed. Prediction models were created for prediction horizon of one hour ahead. Accuracy level of predicted values was compared with prediction results of ANN and GP. The results obtained with the ELM method outperformed the results of the ANN and GP models for both training and testing set of data. It can be concluded that the ELM algorithm can generally be effectively utilized for PET index prediction.

References

[1] Ghasemi, Z., *et al.*, Promotion of Urban Environment by Consideration of Human Thermal & Wind Comfort: A Literature Review, *Procedia Soc. Behav. Sci., 201* (2015), Aug., pp. 397-408
[2] Cohen, P., *et al.*, Daily and Seasonal Climatic Conditions of Green Urban Open Spaces in the Mediterranean Climate and Their Impact on Human Comfort, *Build Environ., 51* (2012), May, pp. 285-295
[3] Taleghani, M., *et al*., A Review into Thermal Comfort in Buildings, *Renew. Sustainable Energy Rev., 26* (2013), Oct., pp. 201-215
[4] Charalampopoulos, I., *et al*., Analysis of Thermal Bioclimate in Various Urban Configurations in Athens, Greece, *Urban Ecosyst., 16* (2013), 2, pp. 217-233
[5] Daneshvar, M., *et al*., Assessment of Bioclimatic Comfort Conditions Based on Physiologically Equivalent Temperature (PET) using the RayMan Model in Iran, *Cent. Eur. J. Geosci*., *5* (2013), 1, pp. 53-60
[6] Salata, T., *et al*., Outdoor Thermal Comfort in the Mediterranean Area. A Transversal Study in Rome, Italy, *Build Environ., 96* (2016), Feb., pp. 46-61
[7] Algeciras, J. A., Matzarakis, A., Quantification of Thermal Bioclimate for the Management of Urban Design in Mediterranean Climate of Barcelona, Spain, *Int. J. Biometeorol., 60* (2015), 8, pp. 1-10
[8] Matzarakis, A., *et al*., Applications of a Universal Thermal Index: Physiological Equivalent Temperature, *Int. J. Biometeorol., 43* (1999), 2, pp. 76-84
[9] ***, Nis-Ortophoto Wider City Area, http://gis.ni.rs/
[10] ***, PUC Institute for Urban Planning Nis, http://www.zurbnis.rs/
[11] ***, Tourist Organization Nis, http://www.visitnis.com
[12] Matzarakis, A., *et al*., Modelling Radiation Fluxes in Simple and Complex Environments – Application of the RayMan Model, *Int. J. Biometeorol., 51* (2007), 4, pp. 323-334
[13] Huang, G. B., *et al*., Extreme Learning Machine: Theory and Applications, *Neurocomputing, 70* (2006), 1, pp. 489-501
[14] Huang, G. B., *et al*., Universal Approximation Using Incremental Constructive Feedforward Networks with Random Hidden Nodes, *IEEE Trans. Neural Netw., 17* (2006), 4, pp. 879-892

Paper submitted: April 19, 2016
Paper revised: August 8, 2016
Paper accepted: September 9, 2016